

# Correlation of Optical Coherence Tomography and Retinal Histology in Normal and Pro23His Retinal Degeneration Pig

Justine Cheng<sup>1</sup>, Elliott H. Sohn<sup>1</sup>, Chunhua Jiao<sup>1</sup>, Kelsey L. Adler<sup>1</sup>, Emily E. Kaalberg<sup>1</sup>, Stephen R. Russell<sup>1</sup>, Robert F. Mullins<sup>1</sup>, Edwin M. Stone<sup>1</sup>, Budd A. Tucker<sup>1</sup>, and Ian C. Han<sup>1</sup>

<sup>1</sup> Carver College of Medicine, Department of Ophthalmology and Visual Sciences, Institute for Vision Research, University of Iowa Hospitals and Clinics, Iowa City, Iowa, USA

**Correspondence:** Ian C. Han, Institute for Vision Research, Department of Ophthalmology and Visual Sciences, University of Iowa Hospitals and Clinics, 200 Hawkins Dr, PFP 11196K; Iowa City, Iowa 52242, USA. e-mail: ian-han@uiowa.edu

**Received:** 26 February 2018

**Accepted:** 23 September 2018

**Published:** 30 November 2018

**Keywords:** optical coherence tomography; retinitis pigmentosa; transgenic animals

**Citation:** Cheng J, Sohn EH, Jiao C, Adler KL, Kaalberg EE, Russell SR, Mullins RF, Stone EM, Tucker BA, Han IC. Correlation of optical coherence tomography and retinal histology in normal and Pro23His retinal degeneration pig. *Trans Vis Sci Tech.* 2018;7(6):18, <https://doi.org/10.1167/tvst.7.6.18>  
Copyright 2018 The Authors

**Purpose:** We correlate optical coherence tomography (OCT) retinal layer thickness measurements with histology in wild-type and retinal degenerative pigs.

**Methods:** OCT scans were obtained using the Bioptigen Envisu R2200. In normal pigs, three eyes were imaged *in vivo*, and three eyes were imaged after enucleation. In the Pro23His retinal degeneration pigs (P23H), one eye was imaged *in vivo* and four eyes were imaged after enucleation. All eyes were fixed in 4% paraformaldehyde and processed for histology. Corresponding retinal locations on OCT and histology were identified using anatomic landmarks (optic nerve, retinal vessels, visual streak). Individual retinal layer thicknesses were measured by two independent, masked graders, and intraclass correlation coefficients were used to determine agreement. OCT and histologic retinal thickness measurements were averaged and compared.

**Results:** OCT and histologic measurements correlated highly in normal and diseased eyes ( $R^2 = 0.91$  and  $0.92$ , respectively), and scans performed *in vivo* and *ex vivo* did not differ significantly. Despite good overall correlation, certain individual retinal layers (e.g., retinal nerve fiber layer [NFL], inner [INL] and outer [ONL] nuclear layers) appeared thicker on OCT compared to histology, while other layers (e.g., retinal pigment epithelium) appeared thinner. No statistically significant difference was found between OCT and histology for any retinal layer thickness measurement.

**Conclusions:** Retinal layer thickness measurements correlate well with histology in pig eyes, but differences in individual retinal layers may be seen.

**Translational Relevance:** OCT may be used in pigs to measure retinal thicknesses with good overall correlation to histologic measurements.

## Introduction

Optical coherence tomography (OCT) is a non-contact, noninvasive imaging modality that is used widely in clinical and research settings to examine detailed retinal structures *in vivo*. Due to its ease of use, OCT has become an indispensable tool for qualitative and quantitative evaluation of retinal anatomy in normal and diseased eyes.<sup>1,2</sup> In animal studies, OCT use has been applied largely to small mammals, such as mice and rats, with limited reports on its use in larger animals such as pigs.<sup>3–5</sup> This is particularly significant because pigs are an ideal model for eye research, possessing similar eye size,

cell distribution, density of cones and spectral cone types, segment morphology, and vascular supply to humans.<sup>6–8</sup> As a result, pigs are accepted as a model organism for many human ophthalmologic conditions, including retinitis pigmentosa (RP) and glaucoma, and are used for preclinical testing of various therapies.<sup>9–12</sup> For example, our group has used the pig for testing the feasibility of induced pluripotent stem cells transplants, as it also is an accepted large animal model for preclinical Food and Drug Administration studies.<sup>13</sup>

Because histologic analysis of pig retinal structures requires sacrifice of the animal and is time-consuming and costly, it is important to identify and validate an imaging method that can accurately and reliably

provide in vivo retinal anatomic measurements. As a proof of concept of the potential of OCT, Gloesmann et al.<sup>14</sup> were able to demonstrate retinal thickness measurements derived from ultra-high resolution OCT imaging in domestic pig eyes. However, this study was performed with an experimental rather than a commercially-available OCT instrument. Moreover, all scans were taken ex vivo after enucleation as well as after dissection of the anterior segment to isolate the retina. To our knowledge, no studies have evaluated in vivo imaging of the pig retina, or demonstrated its use in diseased pig models.

We used a commercially-available OCT system to obtain high quality images of the pig retina in vivo and ex vivo. We further compared measurements of the individual retinal layers and correlated these measurements with those from histology in normal pigs and a disease model of retinal degeneration.

## Methods

### Animals

All animal procedures were approved by the Institutional Animal Care and Use Committee of the University of Iowa and handled in accordance with the Association for Vision Research and Ophthalmology (ARVO) Statement for the Use of Animals in Ophthalmic and Vision Research. Wild-type Yucatan miniature pigs 8 weeks to 6 months old were selected. Six eyes were used in total: three were imaged in vivo (age, 9 weeks–5 months) and three were enucleated and then imaged ex vivo (age, 6–8.5 months). A previously-described transgenic miniature pig model of retinitis pigmentosa, expressing the autosomal dominant Pro23His (P23H) mutation in the gene rhodopsin, also was used in this study.<sup>9</sup> One eye of a 6-week-old pig was imaged in vivo, and three eyes of 7-week-old pigs and one eye of an 8.5-month-old pig were imaged ex vivo.

### OCT Imaging

OCT imaging was performed using the Bioptigen Envisu R2200 (Bioptigen, Inc., Morrisville, NC) spectral-domain OCT system, which has a probe that can be used for hand-held or mounted imaging. The device has an imaging speed of 32,000 A-scans per second and 1.6  $\mu$  axial resolution in tissue. For each eye, scan protocols included 12  $\times$  12 and 6  $\times$  6 mm volume scans centered upon the retina superior to the optic nerve, just above the visual streak. For in vivo scans, anesthesia was induced via intramuscular

injection of ketamine (14 mg/kg) and acepromazine (1 mg/kg), followed by 3% to 4% isoflurane inhalation. Anesthesia subsequently was maintained via inhalation of 1% to 2% isoflurane. The pupils were dilated with 1% tropicamide ophthalmic solution (Alcon, Inc., Ft. Worth, TX) followed by 2.5% phenylephrine hydrochloride ophthalmic solution (Paragon, Kalamazoo, MI). The OCT probe was adapted to an operating microscope using a commercially-available mount (Bioptigen ES100 Surgical Mount) and oriented in a cephalocaudal direction (Fig. 1). After pigs were euthanized by intracardiac injection of sodium phenobarbital (390 mg/10 pounds), the eyes were enucleated. The orientation of the superior retina was determined using a preplaced scleral suture at the superior limbus and confirmation with indirect ophthalmoscopy. OCT imaging was performed using a custom-built platform for positioning of the enucleated eye, and a custom-built adaptor, which was used to mount the OCT probe to a slit-lamp base (Fig. 1). All ex vivo imaging was performed within 10 minutes of enucleation.

### Histologic Preparation

All eyes were immersed in fresh 4% paraformaldehyde immediately after OCT imaging. After 4 hours of fixation, the anterior chamber and vitreous were dissected, and the posterior eyecup was processed for paraffin embedding, using the previously-placed scleral suture at the superior limbus to orient and maintain anatomic orientation of the eye. The tissue was serially sectioned at 10  $\mu$  thickness, and mounted onto Superfrost Plus glass slides (Fisherbrand, Hampton, NH). The anatomic location in the retina between OCT and histology was correlated using anatomic landmarks, including the optic nerve, major arcade vessels, and visual streak (Fig. 2). Corresponding slides from every 100  $\mu$  interval of those locations were selected for hematoxylin and eosin (H&E) staining. Three to five images were captured from each slide after H&E staining using the Olympus BX41 microscope (Olympus America, Inc., Melville, NY).

### Retinal Layer Thickness Measurements

The individual retinal layers were identified using human retina OCT images and domestic pig OCT data published by the Gloesmann et al.<sup>14</sup> and Staurenghi et al.<sup>15</sup> Nine retinal layers were measured, including the nerve fiber layer, ganglion cell layer, inner plexiform layer, inner nuclear layer, outer

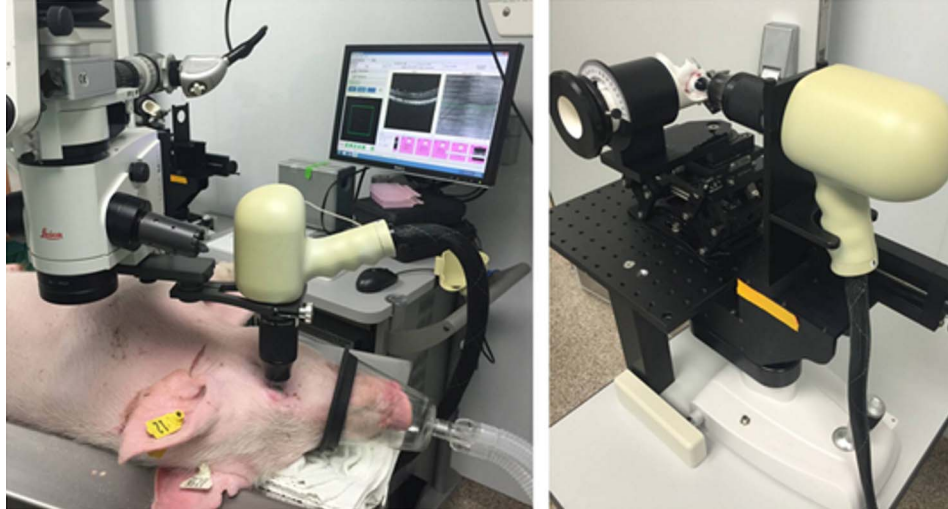


**Figure 1.** Representative photographs of in vivo and ex vivo imaging. *Left:* OCT probe mounted to microscope for in vivo imaging. *Right:* OCT probe attached to custom-built mounts for ex vivo imaging post enucleation.

plexiform layer, outer nuclear layer, photoreceptor inner segment, photoreceptor outer segment, and retinal pigment epithelium (RPE). On the OCT scans, manual retinal thickness measurements were performed in the middle of the horizontal line scans for each individual retinal layer by two masked, independent graders using the caliper tool provided by the software (Biotigen InVivoVue, version 2.4.34; Fig. 3). After determining the corresponding histologic section, the area and length of each retinal layer were

measured using ImageJ (version 1.48, National Institutes of Health, Bethesda, MD). The average thickness then was calculated using these measurements (e.g., area divided by length).

### Statistical analysis

The measurements by two masked, independent graders of the individual retinal layers in histology and OCT were averaged. Intergrader agreement for OCT and histological retinal thickness measurements was determined by intraclass correlation coefficient (ICC). Pearson's correlation coefficients between OCT and histology measurements of each individual retinal layer then were calculated for the following groups: normal (six eyes; three eyes in vivo and three eyes ex vivo) and P23H pigs (five eyes; one eye in vivo, four eyes ex vivo). Differences in histology-OCT correlation between groups were assessed using 2-way analysis of variance (ANOVA) with 1-way ANOVA post hoc testing of each layer.  $P < 0.05$  was considered statistically significant. Statistical calculations were performed using SPSS version 24.0 (IBM Corp., Armonk, NY)

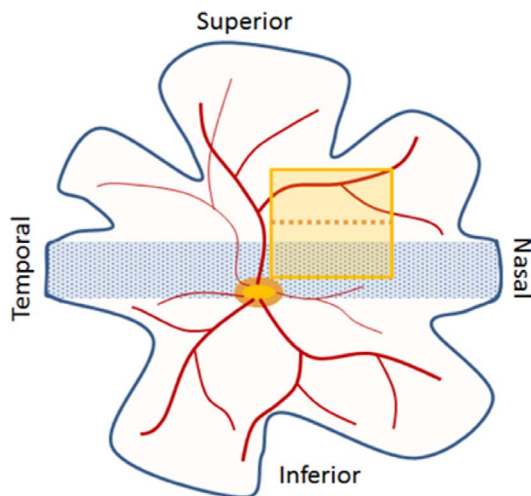


**Figure 2.** Schematic of pig retina and region analyzed. The visual streak is represented by the horizontal light blue rectangle. The area imaged by OCT volume scan is shown in yellow box, with horizontal dotted line showing approximate region used for retinal thickness measurements in comparison to histology.

## Results

### OCT Layer Correlation to Histology in Normal

Intergrader agreement for measurements of the retinal layer thickness was excellent on OCT and

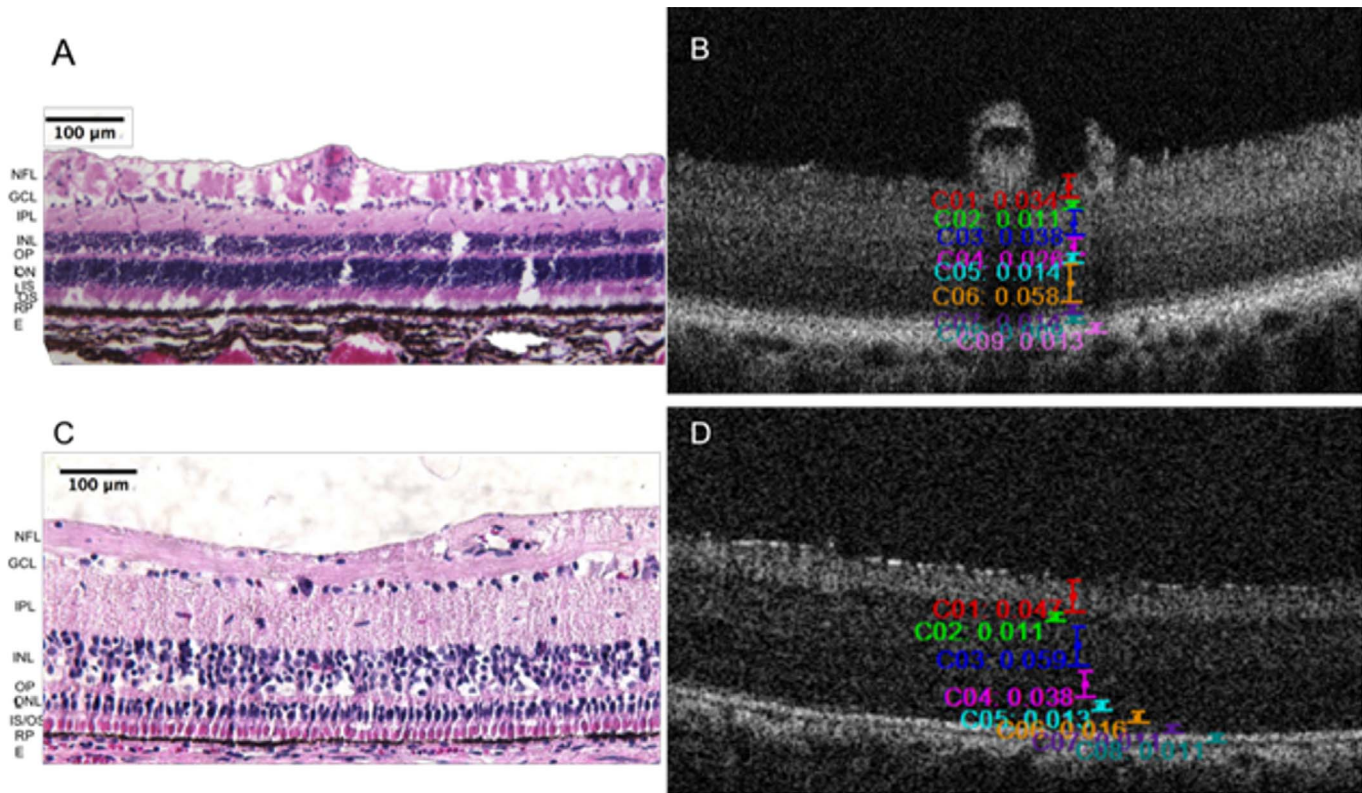


**Figure 3.** Histology and OCT retinal thickness measurements. Representative histologic section (A) and OCT (B) line scan for a normal, wild type Yucatan miniature pig eye. Representative histologic section (C) and OCT (D) for a Pro23His RHO pig eye. Measurements (in millimeters) are shown for individual retinal layers by color-coded calipers (B and D).

histology for all normal pig eyes (ICC, 0.95 and 0.94, respectively). When comparing retinal layer thickness measurements on OCT and histology in all normal eyes, the correlation coefficient was 0.92, suggesting good overall correlation between OCT and histology measurements (Fig. 4A). Although a higher correlation between OCT and histologic data ( $R^2 = 0.96$ ) was identified for measurements of retinal layers obtained before enucleation (i.e., in vivo) than eyes measured after enucleation (i.e., ex vivo;  $R^2 = 0.84$ ), this difference was not statistically significant ( $P = 0.19$ ; Fig. 4B). OCT and histology measurements subsequently were analyzed by individual retinal layers for all normal pig eyes (i.e., in vivo and ex vivo) (Supplementary Table S1). When comparing all normal eyes (in vivo and ex vivo), 2-way ANOVA analysis showed statistically significant differences between OCT and histology of the ganglion cell ( $P = 0.008$ ) and inner nuclear ( $P = 0.006$ ) layers, which on post hoc 1-way ANOVA analysis approached, but did not reach statistical significance ( $P = 0.06$ ,  $P = 0.07$ , respectively). Similarly, a statistically significant difference was found between OCT and histology

for comparison of the ganglion cell layer in vivo ( $P = 0.03$ ), but post hoc analysis revealed no statistically significant difference ( $P = 0.3$ ). A nomogram representing the conversion of individual retinal layer thickness from OCT to histology is shown in Figure 5.

### OCT Layer Correlation to Histology in P23H Pig Model of Retinal Degeneration

As in normal animals, a strong correlation ( $R^2 = 0.92$ ) was found between OCT and histologic measurements for the P23H pig eyes analyzed in vivo ( $R^2 = 0.91$ ) and ex vivo ( $R^2 = 0.92$ ) (Figs. 4D, E). Individual retinal layer thickness measurements were analyzed for all P23H eyes (in vivo and ex vivo). For individual retinal layers, a statistically significant difference between OCT and histology was found in the RPE layer ( $P = 0.03$ ) that was not statistically significant on post hoc analysis ( $P = 0.33$ ). Again, intergrader agreement was excellent for histologic and OCT measurements (ICC, 0.96 and 0.99, respectively).

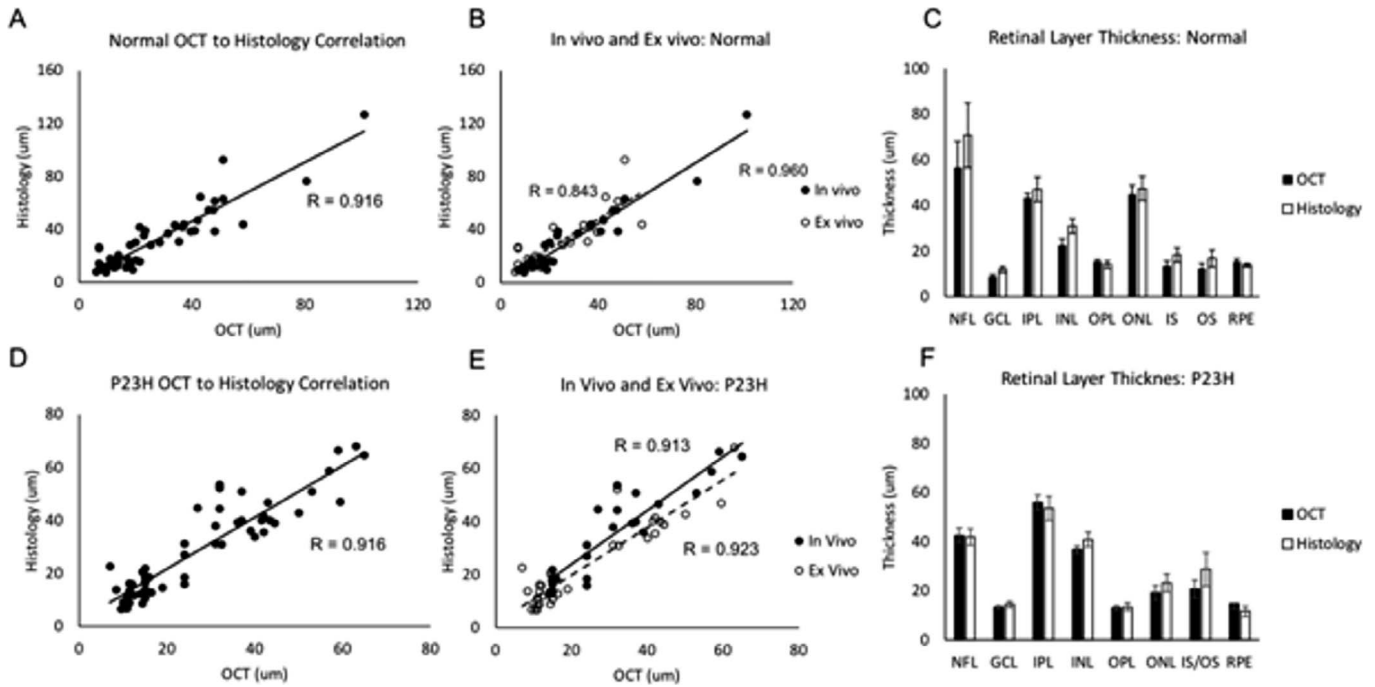


**Figure 4.** Correlation of retinal layer thickness measurements between OCT and histology. Overall OCT to histology correlation of individual retinal layers in normal (A) and P23H (D) pig eyes, with each dot representing retinal layer thickness measurements by OCT and histology, and *R*-value describing the correlation of OCT to histology for all plotted data points. Pig eyes grouped into in vivo (solid dots) and ex vivo (hollow dots) scans for normal (B) and P23H (E) eyes. Thickness measurements of individual retinal layers in normal (C) and P23H (F) pig eyes. GCL, ganglion cell layer; IPL, inner plexiform layer; OPL, outer plexiform layer; IS, photoreceptor inner segment; OS, photoreceptor outer segment.

## Discussion

Our results demonstrated that detailed retinal images of pigs can be obtained using OCT in vivo and ex vivo, and that thickness measurements of individual retinal layers obtained via OCT correlate well with postmortem histologic measurements. Al-

though numerous studies have demonstrated the ability to perform OCT in small animal models, such as mice or rats, limited literature exists on the feasibility and histologic correlation of OCT imaging in pigs. Gloesmann et al.<sup>14</sup> correlated OCT with histology in pigs, but the study used an experimental OCT instrument, and imaging was performed exclusively ex vivo after enucleation, with manipulation of

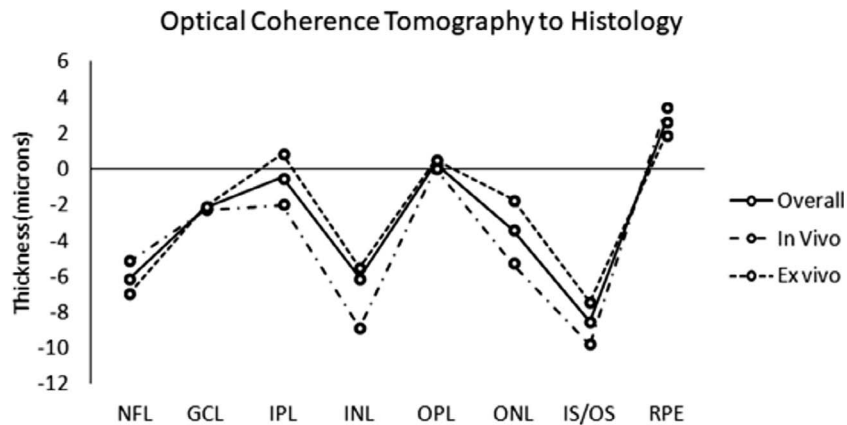


**Figure 5.** Nomogram representing conversion of individual retinal layer thickness from OCT to histology for all eyes (normal and Pro23His pigs) in vivo and ex vivo.

tissue, including removal of the anterior segment, before scan acquisition. In this study, OCT was used successfully *in vivo* and *ex vivo* for normal and retinal degenerative pig eyes. *Ex vivo* imaging was performed after whole eye enucleation, without manipulation of the anterior segment structures and without disturbing the posterior segment structures, thus closely mimicking an *in vivo* setting.

The size of pig eyes is relatively similar to that of human eyes, which makes pig eyes an ideal model for the application and development of surgical techniques and instrumentation. However, it is costly to create pig strains with human retinal genetic disorders, sacrifice pigs, and harvest retinal tissue for histologic studies. Using OCT to detect retinal structures *in vivo* allows monitoring of disease processes as well as treatment effects longitudinally. For example, our group and others are working toward the development of cell replacement therapy using pigs as a large animal model.<sup>13,16</sup> The ability to evaluate retinal structures and obtain reliable measurements of retinal layer thicknesses *in vivo* allows for longitudinal monitoring of any anatomic and structural changes without sacrifice of the animals for each data time point.

This study provides validation of the feasibility of OCT imaging in pigs and demonstrates high correlations of retinal layer thickness measurements between OCT and histology in normal pigs and in a disease model of photoreceptor degeneration (P23H pigs). Although no statistically significant differences between OCT and histologic measurements were detected for any individual retinal layers in our study, measurements of certain retinal layers (e.g., NFL, INL, ONL, photoreceptor inner and outer segments) tended to be thicker on histology than OCT in normal and P23H eyes, whereas certain layers tended to be thicker on OCT (e.g., RPE). The reasons for these differences are unclear, but may be related to tissue changes during fixation for histology, as further discussed below, or from reflectivity changes on OCT that do not represent the true junction between the INL and adjacent layers. For example, in human eyes, ONL may appear thicker on OCT than on histology. This is because the ONL appears hyporeflexive on OCT and is difficult to distinguish from the similarly hyporeflexive overlying Henle's fiber layer, which is much easier to delineate on histology.<sup>15,17,18</sup> Moreover, the reflectivity of certain layers on OCT can be affected by the direction of the scanning laser beam during OCT image acquisition, potentially affecting measurements of retinal layer thickness.<sup>19,20</sup>

Our study demonstrated good correlation of *in vivo* and *ex vivo* OCT measurements with histology in normal and diseased eyes, suggesting that imaging eyes shortly after enucleation (within 10 minutes for this study) may not significantly affect retinal thickness measurements, despite the lack of perfusion *ex vivo*. That said, although not statistically significant, a slightly higher correlation between OCT and histology measurements was identified for the *in vivo* than the *ex vivo* condition for normal eyes. Multiple factors may contribute to variation in OCT layer thickness measurements after enucleation, including perfusion status of the tissue, time from enucleation to imaging, and method of fixation for histology. Further study would be useful to determine the effect of these various factors on OCT–histology correlations. For example, we chose to preserve retinal morphology for histologic analysis by embedding the eyes in paraffin. Certain experiments may require alternate methods of tissue preservation (e.g., frozen section) which may alter tissue differently than paraffin, and may result in different degrees of correlation in retinal thickness measurements between OCT and histology.

This study had several limitations, including its relatively small sample size due to an expensive, large animal model. Our study demonstrated excellent intergrader agreement in the retinal thickness measurements, but these may be more difficult in diseases where numerous retinal layers are disrupted, or where the layers are difficult to distinguish (e.g., in macular edema). In eyes with pathogenic retinal thinning, manual measurement of retinal thicknesses is challenging for layers less than 10  $\mu\text{m}$ , as the calipers on imaging software are more difficult to manipulate. Although *in vivo* imaging may be considered the gold standard for retinal thickness measurements, obtaining high quality pig OCT images *in vivo* can be challenging, as it requires anesthesia and may be affected by factors, such as movement from breathing. Rather than rely upon handheld OCT imaging, we used a commercially-available microscope mount for image acquisition *in vivo* and a custom-built slit-lamp mount for imaging *ex vivo* to obtain high quality images. Qualitatively, we observed that the *ex vivo* imaging scans generally had better quality than those obtained *in vivo*, but *in vivo* and *ex vivo* imaging showed good correlation between OCT and histology in normal eyes. Moreover, images obtained *in vivo* had a higher overall correlation to histology than *ex vivo* scans, suggesting that factors surrounding *ex vivo* imaging, including the lack of ocular

perfusion, may have some effect on retinal thickness measurements and their correlation with histology.

In summary, this study demonstrated the feasibility of in vivo and ex vivo OCT imaging of the pig retina, and high correlation between retinal thickness measurements on OCT and histology in normal and disease miniature pig models. The good correlation demonstrated here provided validity for the use of OCT imaging to evaluate the retinal layers qualitatively and quantitatively in pigs in vivo and ex vivo. However, differences in OCT and histologic measurements of individual retinal layers may be seen, and these differences should be taken into account when comparing measurements between methods of retinal imaging.

## Acknowledgments

Supported by the Institute for Vision Research Endowment, University of Iowa, Iowa City, Iowa, NIH (NEI) P30 EY025580.

Disclosure: **J. Cheng**, None; **E.H. Sohn**, None; **C. Jiao**, None; **K.L. Adler**, None; **E.E. Kaalberg**, None; **S.R. Russell**, None; **R.F. Mullins**, None; **E.M. Stone**, None; **B.A. Tucker**, None; **I.C. Han**, None

## References

- Huang D, Swanson EA, Lin CP et al. Optical coherence tomography. *Science*. 1991;254:1178–1181.
- Gabriele ML, Wollstein G, Ishikawa H., et al., Optical coherence tomography: history, current status, and laboratory work. *Invest Ophthalmol Vis Sci*. 2011;52:2425–2436.
- Rösch S, Johnen S, Müller F, Pfarrer C, Walter P. Correlations between ERG, OCT, and Anatomical Findings in the rd10 Mouse. *J Ophthalmol*. 2014;2014:874751.
- Knott EJ, Sheets KG, Zhou Y, Gordon WC, Bazan NG. Spatial correlation of mouse photoreceptor-RPE thickness between SD-OCT and histology. *Exp Eye Res*. 2011;92:155–160.
- Berger A, Cavallero S, Dominguez E, et al. Spectral-domain optical coherence tomography of the rodent eye: highlighting layers of the outer retina using signal averaging and comparison with histology. *PLoS One*, 2014;9:e96494.
- Stricker-Krongrad A, Shoemaker CR, Bouchard GF. The miniature swine as a model in experimental and translational medicine. *Toxicol Pathol*. 2016;44:612–623.
- McLellan GJ, Rasmussen CA. Optical coherence tomography for the evaluation of retinal and optic nerve morphology in animal subjects: practical considerations. *Vet Ophthalmol*. 2012.; 15(suppl 2):13–28.
- Sanchez I, Martin R, Ussa F, Fernandez-Bueno U. The parameters of the porcine eyeball. *Graefes Arch Clin Exp Ophthalmol*. 2011;249:475–482.
- Ross JW, Fernandez de Castro JP, Zhao J, et al. Generation of an inbred miniature pig model of retinitis pigmentosa. *Invest Ophthalmol Vis Sci*. 2012;53:501–507.
- Sommer JR, Wong FL, Petters RM. Phenotypic stability of Pro347Leu rhodopsin transgenic pigs as indicated by photoreceptor cell degeneration. *Transgenic Res*. 2011;20:1391–1395.
- Ruiz-Ederra J, Garcia M, Hernandez M, et al. The pig eye as a novel model of glaucoma. *Exp Eye Res*. 2005;81:561–569.
- Sommer JR, Estrada JL, Collins EB, et al. Production of ELOVL4 transgenic pigs: a large animal model for Stargardt-like macular degeneration. *Br J Ophthalmol*. 2011;95:1749–1754.
- Sohn EH, Jiao C, Kaalberg E, et al. Allogenic iPSC-derived RPE cell transplants induce immune response in pigs: a pilot study. *Sci Rep*. 2015;5:11791.
- Gloesmann M, Hermann B, Schubert C, et al. Histologic correlation of pig retina radial stratification with ultrahigh-resolution optical coherence tomography. *Invest Ophthalmol Vis Sci*. 2003;44:1696–1703.
- Staurengi G, Sadda S, Chakravarthy U, et al. Proposed lexicon for anatomic landmarks in normal posterior segment spectral-domain optical coherence tomography: the IN\*OCT consensus. *Ophthalmology*, 2014;121:572–578.
- Koss MJ, Fallabella P, Stefanini FR, et al. Subretinal implantation of a monolayer of human embryonic stem cell-derived retinal pigment epithelium: a feasibility and safety study in Yucatan minipigs. *Graefes Arch Clin Exp Ophthalmol*. 2016; 254;8:1553–1565.
- Ouyang Y, Walsh AC, Keane PA, et al. Different phenotypes of the appearance of the outer plexiform layer on optical coherence tomography. *Graefes Arch Clin Exp Ophthalmol*. 2013;251: 2311–2317.
- Cuenca N, Ortuno-Lizaran I, Pinilla I. Cellular characterization of OCT and outer retinal bands

- using specific immunohistochemistry markers and clinical implications. *Ophthalmology*, 2018; 125:407–422.
19. Lujan BJ, Roorda A, Knighton RW, Carroll, J. Revealing Henle’s fiber layer using spectral domain optical coherence tomography. *Invest Ophthalmol Vis Sci*. 2011;52:1486–1492.
  20. Lujan BJ, Roorda A, Croskrev JA, et al. Directional optical coherence tomography provides accurate outer nuclear layer and henle fiber layer measurements. *Retina*, 2015;35:1511–1520.